ACTA STEREOL 1992; 12/1: 41-48
ORIGINAL SCIENTIFIC PAPER

ON INTERPRETING A DISTRIBUTION OF RANDOM INTERLAMELLAR DISTANCE INVERSE IN CASE OF PEARLITE

Andrzej Czarski, Kazimierz Satora, Jerzy Ryś

Institute of Metallurgy, Academy of Mining and Metallurgy,
Al.Mickiewicza 30, Cracow, Poland.

ABSTRACT

A simple model of lamellar structure and a method for interpreting distribution of random interlamellar distance inverse are presented. Theoretical considerations are compared with experimental results. As a material for experiments pearlite (lamellar structure being a product of eutectoid reaction in Fe–C system) has been chosen. The results obtained are thoroughly discussed and compared with those for a model lamellar structure.

Keywords: distance distribution inverse, interlamellar distance distribution, lamellar structure, pearlite, random interlamellar distance, true interlamellar distance.

INTRODUCTION

Pearlite is a product of eutectoid reaction in Fe–C system. A growth interaction between ferrite and cementite grains forms a microstructure with lamellar morphology (Hillert 1962, Hackney and Shiflet 1987, Doi and Kestenbach 1989). Lamellar morphology of parallell ferrite and cementite platelets in large colonies is dominating. Local deviations, like fibre–shaped cementite, rapid changes in platelet growth direction, disturbances in vicinity of non–metallic inclusions etc. are considered as growth or structural errors (Bramfitt and Marder 1973, Frank and Puttick 1956, Bolling and Richman 1970, Kirkaldy and Sharma 1980).
In the current approach a method for interpreting distribution of random interlamellar distance inverse is presented. The results of experiments are compared with those obtained for a model lamellar structure. The results presented are included in a large research project devoted to kinetics of eutectoid reaction and spheroidization process.

STEREOLOGICAL DESCRIPTION OF A LAMELLAR STRUCTURE

Quantitative parameters of lamellar structures i.e. true (l_t), apparent (l_a) and random (l_r) interlamellar distances have been proposed by Underwood in DeHoff and Rhines (1968) and Underwood (1970). It should be stressed that in fact parameters of a model lamellar structure which is more or less simplified, are evaluated. Therefore it

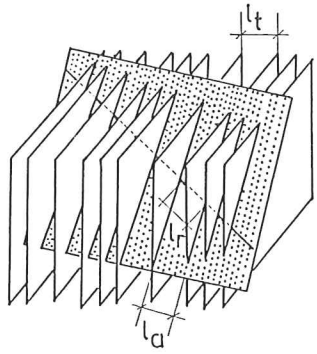

Fig.1. Model lamellar structure

is important to analyse the adequacy between model and real metallographic lamellar structures. Let us consider a model lamellar structure (see Fig.1) and analyse relation between a distribution of random interlamellar distance (and its inverse) and a distribution of true interlamellar distance. Conditional density functions for the distribution of random distance and its inverse are given as (Czarski and Ryś 1987,1990):

$$f(l_r|l_t) = \frac{l_t}{l_r^2}; \quad l_t \le l_r < \infty \tag{1}$$

$$f(l_r^{-1}|l_t) = l_t; \quad 0 < l_r^{-1} \le l_t^{-1} \tag{2}$$

Taking into consideration function (1) and solving equation

$$f(l_r) = \int_0^{l_r} f(l_r|l_t)\, f(l_t)\, dl_t \tag{3}$$

we get

$$f(l_t)_{l_t=l_r} = 2f(l_r) + l_r \frac{df(l_r)}{dl_r} \tag{4}$$

where: $f(l_r)$, $f(l_t)$ – density functions for random and true interlamellar spacing, respectively.

A similar analysis according to the density function for random interlamellar spacing inverse $f(l_r^{-1})$ will be performed only for density functions $f(l_t)$ positively defined in a closed interval $l_t \in \langle l_{tmin}, l_{tmax} \rangle$ (other cases have no practical significance). For such cases we can derive from (2):

$$f(l_r^{-1}) = \begin{cases} \int_{l_{tmin}}^{l_{tmax}} l_t\, f(l_t)\, dl_t = const; & 0 < l_r^{-1} < l_{tmax}^{-1} \\ \int_{l_{tmin}}^{l_r} l_t\, f(l_t)\, dl_t; & l_{tmax}^{-1} < l_r^{-1} \le l_{tmin}^{-1} \end{cases} \tag{5}$$

Analysis of expression (5) shows that if function $f(l_t)$ is (as assumed) positively defined in a closed interval, then, irrespective of its form, function $f(l_r^{-1})$ will take a constant value in the interval $0 < l_r^{-1} \le l_{tmax}^{-1}$. In other words a plateau will be visible in the plot of this function.

Due to the presence of plateau mentioned above distribution of the random spacing inverse becomes practically important as it can be used for verifying the introduced

model and (in case of its correctness) for estimation of the maximum real interlamellar spacing.
The following example will illustrate the whole analysis. Let us assume that the distribution of true interlamellar spacing is given by function (6):

$$f(l_t) = \frac{1}{l_{t\max} - l_{t\min}} \tag{6}$$

Taking (3) and (5) we obtain respectively:

$$f(l_r) = \begin{cases} \frac{1}{2(l_{t\max} - l_{t\min})}\left(1 - \frac{l_{t\min}^2}{l_r^2}\right); & l_{t\min} \le l_r < l_{t\max} \\ \frac{1}{2\,l_r^2}\left(l_{t\max} + l_{t\min}\right); & l_{t\max} \le l_r < \infty \end{cases} \tag{7}$$

and

$$f(l_r^{-1}) = \begin{cases} \frac{1}{2}\left(l_{t\max} + l_{t\min}\right); & 0 < l_r^{-1} \le l_{t\max}^{-1} \\ \frac{1}{2\,(l_{t\max} - l_{t\min})}\left[(l_r^{-1})^{-2} - l_{t\min}^2\right]; & l_{t\max}^{-1} < l_r^{-1} \le l_{t\min}^{-1} \end{cases} \tag{8}$$

Plots of functions (6), (7) and (8) for selected values of l_{tmin} and l_{tmax} are shown in Figs 2, 3 and 4, respectively.

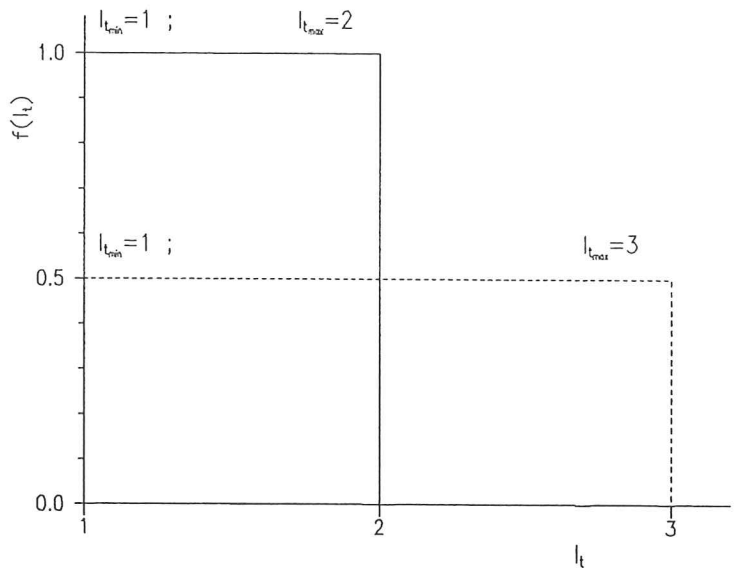

Fig.2. Distribution of true interlamellar spacing (6);
continuous line for l_{tmin}=1, l_{tmax}=2;
broken line for l_{tmin}=1, l_{tmax}=3.

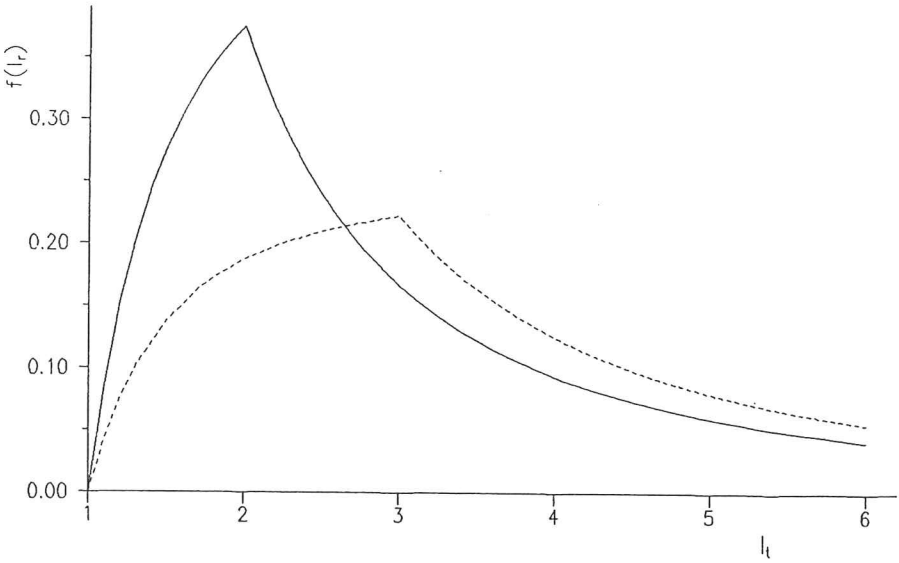

Fig.3. Distribution of random interlamellar spacing (7);
continuous line for $l_{tmin}=1$, $l_{tmax}=2$;
broken line for $l_{tmin}=1$, $l_{tmax}=3$.

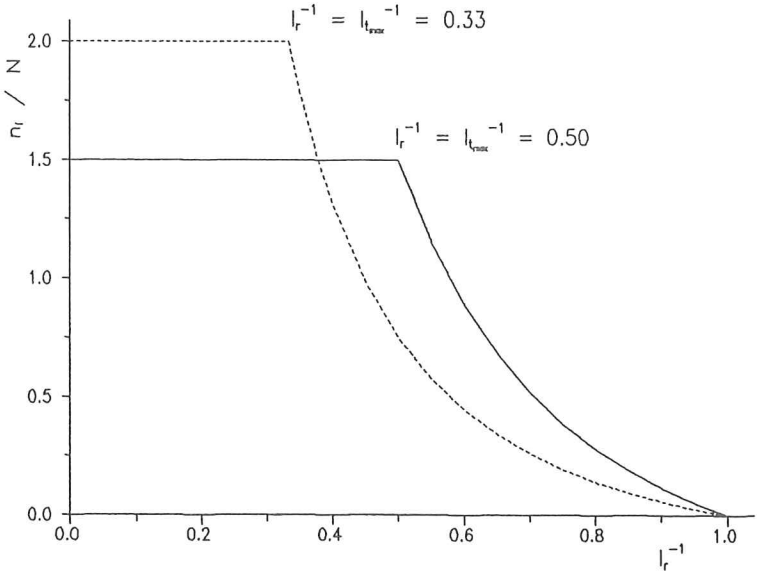

Fig.4. Distribution of random interlamellar spacing inverse (8);
continuous line for $l_{tmin}=1$, $l_{tmax}=2$;
broken line for $l_{tmin}=1$, $l_{tmax}=3$.

EXPERIMENTAL PROCEDURE

A high–purity model Fe–C alloy and carbon 0.8%C steel (grade N8E) have been used for experiments (see Table 1). The pearlitic microstructure has been obtained in the following way:

model alloy – austenitizing 900°C for 30 min.; isothermal annealing 700°C for 3 h,

carbon steel – austenitizing 900°C for 30 min.; isothermal annealing 690°C for 3 h.

Table 1. Chemical composition of the material tested (wt %)

material	C	Mn	Si	P	S	Cr	Ni	Cu	Al	N
model alloy	0.80	0.06	0.00	0.003	0.010	0.04	0.03	traces	0.01	0.006
carbon steel	0.83	0.28	0.20	0.014	0.015	0.04	0.06	0.06	–	–

Microstructures have been examined using optical microscope and are shown in Figs 5 and 6. Distributions of random spacing and random spacing inverse have been evaluated on both materials at total magnification x2500. The results of experiments are shown in Fig.7, Fig.8 and Table 2.
It should be stressed that for l_r^{-1} values greater than $1.25*10^{-3}$ (classes 11 and 12 in Table 2), due to the limited accuracy of single measurements it was impossible to analyse the experimental distribution more accurately. Therefore classes 11 and 12 in Table 2 are significantly wider than classes 1–10.

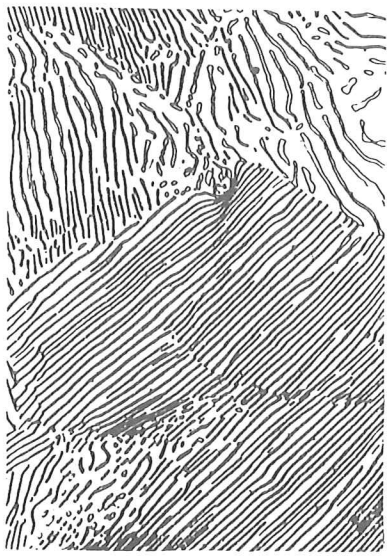

Fig.5. Microstructure of the pearlite in carbon steel used in experiments.

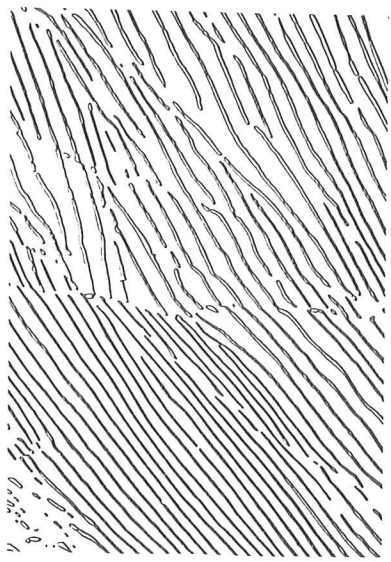

Fig.6. Microstructure of the pearlite in model alloy used in experiments.

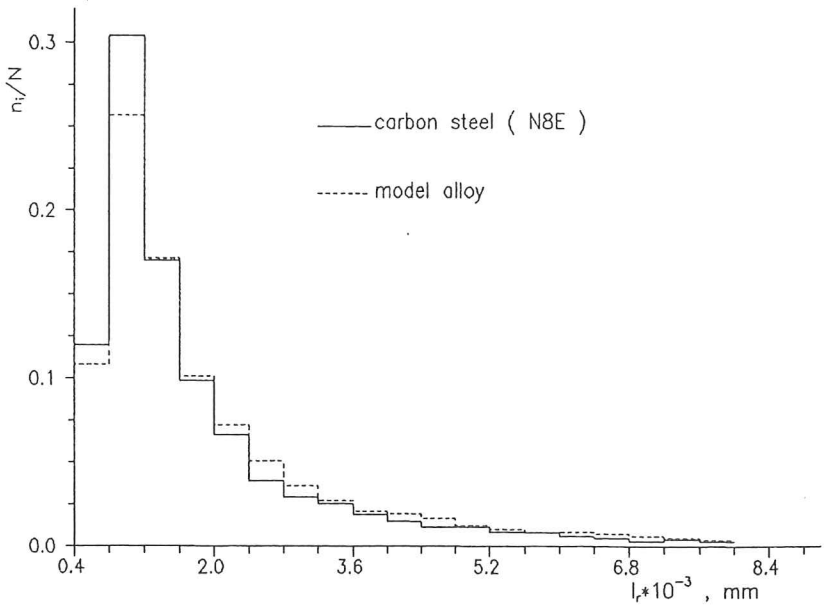

Fig.7. Experimental distribution of random interlamellar spacing.
Continuous line – carbon steel; broken line – model alloy.

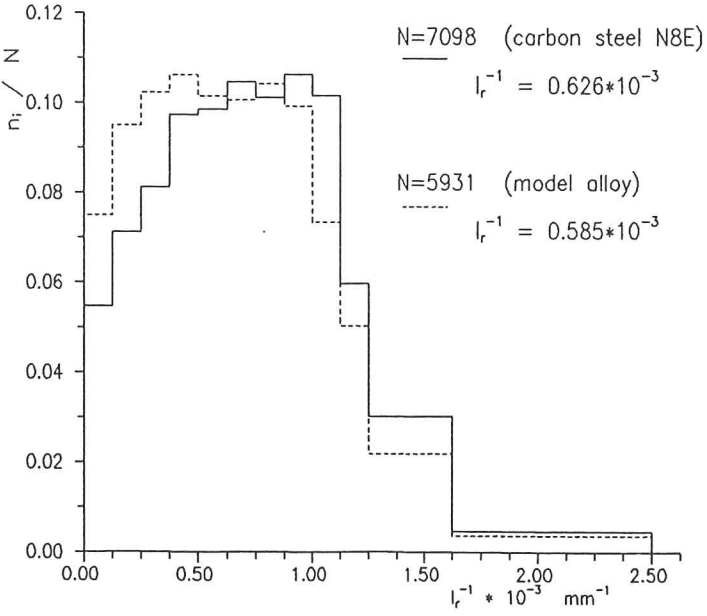

Fig.8. Experimental distribution of random interlamellar spacing inverse
Continuous line – carbon steel; broken line – model alloy.

Table 2. Experimental distribution of l_r^{-1}

class intervals 10^{-3} [mm]	class number	carbon steel			model alloy		
		count	relative frequency	range	count	relative frequency	range
0.000–0.125	1	389	0.05480		445	0.07503	
0.125–0.250	2	506	0.07129	*I*	564	0.09509	*I*
0.250–0.375	3	577	0.08129		607	0.10234	
0.375–0.500	4	691	0.09735		630	0.10622	
0.500–0.625	5	700	0.09862		602	0.10150	
0.625–0.750	6	744	0.10482	*II*	598	0.10083	*II*
0.750–0.875	7	719	0.10129		619	0.10437	
0.875–1.000	8	755	0.10637		589	0.09931	
1.000–1.125	9	722	0.10172		436	0.07351	
1.125–1.250	10	425	0.05988		299	0.05041	
1.250–1.625	11	644	0.09073	*III*	391	0.06593	*III*
1.625–2.500	12	226	0.03184		151	0.02546	
Total		7,098	1.0		5,931	1.0	

DISCUSSION

Only stereological aspects of the distributions discussed will be analysed in this section, with no comments concerning metallography. As it has been predicted in the random spacing inverse distribution (Fig.4) there should be observed a plateau (see eqn.(1)). Identification of this plateau is essential to verify the model proposed. For comparison of the two experimental distributions it seems to be important to notice that there is no significant difference in total counts for both distributions (7098 and 5931, respectively).

In both distributions one can observe three characteristic ranges, denoted in Table 2 by *I, II* and *III*. In range *II* we have a clear plateau; it would be in perfect agreement with the model except for the non–uniform distribution in range *I*. Let us try to explain this unexpected behaviour in range *I*. It seems that the reason is twofold: it is connected with (1) measurements and (2) structure properties.

Measurements. Range *I* and especially class 1 is evaluated from the largest l_r values. These large values are met relatively rarely and therefore the whole result is extremely number–of–measurements sensitive. Thus, even in the case of a perfectly correct and precise model such disturbances could be observed, especially in the class 1.

Structure properties. The above discussion does not explain, however, why it is more difficult to obtain plateau in the case of carbon steel (plateau is visible from class 4 – compare Table 2). The possible solution lies in the clearly visible fact (see Fig.5 and 6) that lamellar morphology of pearlite in carbon steel is less regular than in model alloy. In other words, pearlitic structure of the model alloy is in better agreement with the model introduced (see Fig.1).

Before skipping to the third range (*III*) it is essential to decide if the discrepancies between model and results of measurements are small enough to accept the model. The answer is "yes" because:
(1) errors in class 1 occur mainly due to the technique of measurements, as it has been explained above,
(2) experimental results from class 1 are generally meaningless for reconstruction of the true spacing distribution. This last item is discussed in details by Czarski and Ryś (1991).
When we accept the model proposed it can be stated that the boundary value between ranges *II* and *III* represents the maximum of interlamellar spacing inverse ($l_{tmax}^{-1} = 1.125*10^{-3}$ [mm] for model alloy and $l_{tmax}^{-1} = 10^{-3}$ [mm] for carbon steel). Additionally the form of range *III* will be determined by the distribution of true interlamellar spacing in the structure. The difference in l_{tmax}^{-1} values (smaller value for model alloy) can be easily physically explained as pearlitic reaction requires smaller surfusion for this material.

REFERENCES

Bolling GF, Richman RH. Forced velocity pearlite. Metal Trans 1970; 1: 2095–104.
Brambfitt BL, Marder AR. A transmission–electron–microscopy study of the substructure of high–purity pearlite. Metallography 1973; 6: 483–95.
Czarski A, Ryś J. Stereological relationships for lamellar structure. Acta Stereol 1987; 2: 567–72.
Czarski A, Ryś J. Estimation of true interlamellar spacing in pearlite. Acta Stereol 1991; 1: 25–35.
DeHoff RT, Rhines FN. Quantitative microscopy. McGraw–Hill Book Co. New York 1968.
Doi SN, Kestenbach H–J. Determination of the pearlite nodule size in eutectoid steels. Metallography 1989; 23: 135.
Frank FC, Puttick KE. Cementite morphology in pearlite. Acta Metall 1956; 4: 206–10.
Hackney SA, Shiflet GJ. Pearlite growth mechanism. Acta Metall 1987; 35: 1019.
Hillert M. The formation of pearlite. In: Decomposition of austenite by diffusional processes. Zakay VF, Aaronson HI, eds. Interscience, New York 1962; 197–247.
Kirkaldy JS, Sharma RC. Stability principles for lamellar eutectoid (ic) reactions. Acta Metall 1980; 28: 1009–21.
Underwood EE. Quantitative stereology. Addison–Wesley; Reading 1970.

Received: 1993-02-19
Accepted: 1993-05-26